Crosstalk between the ubiquitin–proteasome system and autophagy in a human cellular model of Alzheimer's disease

Valentina Cecarini [a,*], Laura Bonfili [a], Massimiliano Cuccioloni [a], Matteo Mozzicafreddo [a], Giacomo Rossi [b], Laura Buizza [c], Daniela Uberti [c], Mauro Angeletti [a], Anna Maria Eleuteri [a]

[a] School of Biosciences and Biotechnology, University of Camerino, 62032 Camerino, Italy
[b] School of Medical Veterinary Sciences, University of Camerino, 62024 Matelica, Italy
[c] Dept. Biomedical Science and Biotechnologies, University of Brescia, 25123 Brescia, Italy

ARTICLE INFO

ABSTRACT

Alzheimer's disease is the most common progressive neurodegenerative disorder characterized by the abnormal deposition of amyloid plaques, likely as a consequence of an incorrect processing of the amyloid-β precursor protein (AβPP). Dysfunctions in both the ubiquitin–proteasome system and autophagy have also been observed. Recently, an extensive cross-talk between these two degradation pathways has emerged, but the exact implicated processes are yet to be clarified. In this work, we gained insight into such interplay by analyzing human SH-SY5Y neuroblastoma cells stably transfected either with wild-type AβPP gene or 717 valine-to-glycine AβPP-mutated gene. The over-expression of the AβPP mutant isoform correlates with an increase in oxidative stress and a remodeled pattern of protein degradation, with both marked inhibition of proteasome activities and impairment in the autophagic flux. To compensate for this altered scenario, cells try to promote the autophagy activation in a HDAC6-dependent manner. The treatment with amyloid-β_{42} oligomers further compromises proteasome activity and also contributes to the inhibition of cathepsin-mediated proteolysis, finally favoring the neuronal degeneration and suggesting the existence of an Aβ_{42} threshold level beyond which proteasome-dependent proteolysis becomes definitely dysfunctional.

© 2012 Elsevier B.V. All rights reserved.

1. Introduction

Alzheimer's disease (AD) is a progressive neurodegenerative disorder pathologically characterized by the neurofibrillary tangles of hyperphosphorylated tau protein, amyloid-β plaques and loss of neurons and synapses in specific brain regions [1]. These plaques are formed mostly by 40 and 42 amino acid long peptides (Aβ_{40} and Aβ_{42}, respectively), derived from the proteolytic cleavages of the amyloid precursor protein (AβPP) [1]. Considering the centrality of AβPP in the generation of the amyloid peptides, it is clear that alterations in the AβPP pathway may directly contribute to the disease pathogenesis [2]. Previous studies suggested a role for the proteasome and lysosomes in AβPP processing, indicating that an impairment in their activity can favor the onset of the disorder [3,4]. The 26S proteasome is a large, barrel shaped protease complex in charge of the removal of intracellular misfolded, oxidized or aggregated proteins in the presence of ubiquitin (Ub) and ATP. The catalytic core of this structure is the 20S proteasome, possessing four well characterized proteolytic activities [5]. Numerous data demonstrated that AD and other neurodegenerations are characterized by an impaired functionality of the Ub–proteasome system (UPS) and that amyloid aggregates are able to inhibit such complex [6–8]. Furthermore, it was also reported that proteasome inhibition altered AβPP processing, modulating Aβ production [3,9]. Differently, lysosomes are responsible for the degradation and recycling of intracellular components through autophagic pathways [10]. Autophagy is crucial for both neuronal homeostasis and survival during nutrient starvation, hence damages in the autophagic flux promote severe cellular alterations with the accumulation of abnormal proteins and/or damaged organelles [11]. The lysosomal enzymes cathepsin B and cathepsin L can interfere with AβPP processing, thus altering the Aβ release [12]. The in vivo treatment with a cathepsin B inhibitor of London APP mice, an AD model expressing human APP containing the wt β-secretase site and mutation at the γ-secretase, improved memory function, reduced amyloid plaque load, decreased Aβ_{40} and Aβ_{42}, and reduced β-secretase-cleaved AβPP C-terminal fragments [13].

An extensive cross-talk between the proteasomal system and lysosomal degradation has been documented [14,15], but the exact mechanisms implicated in such cooperation have to be better clarified. On this regard, the histone deacetylase 6 (HDAC6) deserves attention being not only dedicated to genomic functions, but also involved in cytoplasmic pathways. This enzyme includes a Ub-binding domain that associates

with the microtubules and actin cytoskeleton, which contributes both to aggresome formation, favoring the transport of ubiquitinated misfolded proteins through microtubules, and to aggresome clearance [16,17]. HDAC6 regulates Hsp90 functions through reversible acetylation, thus its inactivation triggers Hsp90 hyperacetylation, with the resulting loss of chaperone activity [18]. Pandey et al. found that compensatory autophagy was induced in *Drosophila melanogaster* in a HDAC6-dependent manner in response to mutations affecting the proteasome, suggesting that damages to the autophagic pathway might predispose to neurodegenerative processes [15,19].

Here, we dissected the regulation of the two proteolytic systems in Alzheimer's disease using human SH-SY5Y neuroblastoma cells stably transfected with either wild-type AβPP gene (APPwt) or 717 valine-to-glycine AβPP-mutated gene (APPmut) as experimental model. Our data show that the over-expression of the amyloid precursor protein correlates with an increase in oxidative stress and with a reorganization of the cellular proteolytic machineries. Additionally, we identify the HDAC6-increased expression as a cellular attempt to activate compensatory autophagy in such altered scenario. The further increase in $A\beta_{42}$ levels undeniably compromises proteasome activity and contributes to the inhibition of cathepsins, finally favoring the neuronal degeneration.

2. Material and methods

2.1. Reagents and chemicals

Substrates for assaying the chymotrypsin-like (ChT-L), trypsin-like (T-L), peptidylglutamyl-peptide hydrolyzing (PGPH), aminopeptidase N (AP-N) activities and proteasome inhibitors, Z-Gly-Pro-Phe-Leu-CHO and lactacystin, were purchased from Sigma-Aldrich S.r.L. (Milano, Italy). The substrate Z-Gly-Pro-Ala-Phe-Gly-pAB to test the branched-chain amino acids preferring (BrAAP) activity was a kind gift from Prof. Orlowski (Department of Pharmacology, Mount Sinai School of Medicine, New York, USA). Aminopeptidase N (EC 3.4.11.2) for the coupled assay utilized to detect BrAAP activity [20], was purified from pig kidney as reported elsewhere [21]. Cathepsin B and cathepsin L substrates (Z-Arg-Arg-AMC and Z-Phe-Arg-AFC.trifluoroacetate) and inhibitors (CA074Me and N-(1-Naphthalenylsulfonyl)-Ile-Trp-aldehyde) were obtained from Sigma-Aldrich S.r.L. (Milano, Italy). Lyophilized $A\beta_{42}$ was purchased from Invitrogen and stored as powder at −20 °C until reconstitution in hexafluoroisopropanol (HFIP). Media and chemicals used for cell cultures were purchased from Enzo Life Sciences, Inc. NuPAGE® Novex 12% Bis-Tris gels for SDS-PAGE were purchased from Invitrogen (Milano, Italy). Membranes for western blotting analyses were purchased from Millipore (Milano, Italy). Proteins immobilized on films were detected with the enhanced chemiluminescence (ECL) system (Amersham Pharmacia Biotech, Milano, Italy).

2.2. Cell culture and transfections

SH-SY5Y cells were cultured in 1:1 Dulbecco's modified Eagle's medium and Nutrient Mixture F12 containing 10% fetal bovine serum (FBS), 2 mM glutamine, 100 units/mL penicillin, and 100 μg/mL streptomycin at 37 °C in a 5% CO_2-containing atmosphere. The SH-SY5Y cell stable transfection with wild type AβPP 751 (APPwt) and AβPP (Val717Gly) mutations (APPmut), was prepared as follows. Cells, seeded on polylysine-coated 6-well plate at 80% of confluence density, were transfected with 1 μg/well of pcDNA–APP751 vector or 1 μg/well of pcDNA–APP751(Val717Gly) mutation vector using Lipofectamine™ 2000 reagent (Invitrogen, Milano, Italy). G418 was added at a concentration of 800 μg/mL and drug resistant cells were collected after 2–3 weeks for single cell cloning; transfected cells were diluted, and seeded in 96-well plates at one cell per well. Wells containing more than 1 cell were marked and excluded from further investigation. 50% medium in each well was replaced twice a week. After 4–6 weeks,

surviving clones reached confluence and were expanded for banking. Resistant clones were analyzed by western blotting to confirm the AβPP overexpression. Stable transfected cells expressing either the APPwt or the APPmut construct were maintained in G418 at a final concentration of 300 μg/mL.

2.3. Preparation of cellular lysates and western blotting

After removing the medium and washing with cold phosphate buffered saline (PBS), cells were harvested in 4 mL of PBS and centrifuged at $1600 \times g$ for 5 min. The pellet was resuspended in a lysis buffer (20 mM Tris, pH 7.4, 250 mM sucrose, 1 mM EDTA and 5 mM β-mercaptoethanol) and passed through a 29-gauge needle at least ten times. Lysates were centrifuged at $12,000 \times g$ for 15 min and the supernatants were stored at −80 °C. Protein concentration was determined by the method of Bradford [22] using bovine serum albumin (BSA) as standard. Cell lysates were then resolved by 12% SDS-PAGE and electroblotted onto PVDF membranes. Membranes with transferred proteins were incubated with primary monoclonal antibodies and successively with the specific peroxidase-conjugated secondary monoclonal antibodies (Abcam, Cambridge, UK). The immunoblot detection was performed with an ECL western blotting analysis system. Each gel was loaded with molecular mass markers, in the range of 6.5 kDa to 205 kDa (SigmaMarker − Wide Molecular Weight Range; Sigma-Aldrich S.r.l.). Glyceraldehyde-3-phosphate dehydrogenase (GAPDH) or α-tubulin was utilized as control for equal protein loading: membranes were stripped and re-probed for GAPDH or α-tubulin using a monoclonal antibody diluted 1:500 (Santa Cruz Biotech, Heidelberg, Germany). The bands were quantified as reported elsewhere [23].

2.4. Detection of autophagic markers

For the immunofluorescence analysis of LC3, cells were serum starved for 4, 6 and 8 h and fixed in 1:1 (v/v) methanol and acetic acid for 5 min at −20 °C. After washing with PBS, cells were labeled with the anti-LC3 monoclonal antibody in PBS containing 1% BSA. Fluorescein-conjugated secondary antibody was used. Cells were stained with Hoechst dye and then slides were mounted with Moviol and examined using a fluorescence microscope. Quantitative analysis was performed by counting the number of LC3 positive dots in six different fields/slices. Nearly 20 cells/field were counted. For each sample, at least, three different slices were evaluated. The state of the autophagic flux was assessed upon 8 h of serum deprivation through western blotting assays with specific primary antibodies detecting the levels of autophagy related proteins such as LC3-II, beclin-1 (both antibodies purchased from Pierce Biotech, Rockford, USA) and p62 (antibody purchased from Sigma-Aldrich, Milano, Italy) and the amount of Ub–protein conjugates (monoclonal anti-Ub antibody purchased from Santa Cruz Biotechnology, Inc. Heidelberg, Germany).

2.5. Cell viability

Cell viability was determined by 3-(4,5-dimethylthiazol-2-yl)-2,5-diphenyltetrazolium bromide (MTT) conversion as previously described [24]. Briefly, following experimental treatment, cells were washed in PBS, pH 7.5, and then MTT (final concentration 0.5 mg/mL) was added to the culture medium without FBS and incubated for 2 h at 37 °C. The medium was then removed and replaced with 100 μL of DMSO. The optical density was measured at 550 nm in a microtiter plate reader. At least six cultures were utilized for each time point.

2.6. Quantification of protein carbonyls (PC)

Protein carbonyls were determined as described in Prof. Butterfield's laboratory [25]. Samples were treated following the procedure of the OxyBlot™ protein oxidation detection kit (Chemicon Millipore, Billerica,

MA, USA). Derivatized proteins were blotted onto a nitrocellulose membrane with a dot-blot apparatus (2 μg per dot) in quadruplicate. The membrane was blocked with a solution of 5% non-fat dried milk in Tris-buffered saline (TBS) solution and followed by incubation with rabbit polyclonal anti-DNPH antibody (1:100) as primary antibody for 1 h at room temperature. After washing, the membrane was incubated with HRP-conjugated goat anti-rabbit secondary antibody (1:300) for 1 h at room temperature. Blots were developed using a chemiluminescence blotting substrate kit and densitometric analysis was performed using Scion Image software (Scion Corporation). Data were normalized to α-tubulin.

2.7. Quantification of 3-nitrotyrosine (3-NT)

The 3-NT content was determined immunochemically as previously described [26]. Briefly, samples were incubated with Laemmli sample buffer in a 1:2 ratio (0.125 M Trizma base, pH 6.8, 4% SDS, 20% glycerol) for 20 min. Proteins (5 μg) were then blotted in quadruplicate onto the nitrocellulose paper using the slot-blot apparatus and immunochemical methods were conducted as described above for protein carbonyls. The rabbit anti-3-NT primary antibody (1:1000 dilution) (Sigma-Aldrich, Milano, Italy) was incubated overnight at 4 °C and at room temperature for 3 h. Next, the HRP-conjugated goat anti-rabbit secondary antibody (1:1500, Dako, Glostrup, Denmark) was incubated for 2 h at room temperature. Densitometric analysis was performed using Scion Image software. Data were normalized to α-tubulin.

2.8. Quantification of 4-hydroxynonenal (HNE)

Detection of HNE adducts was performed as follows. Samples (5 μg) were incubated with Laemmli buffer containing 0.125 M Tris base pH 6.8, 4% (v/v) SDS, and 20% (v/v) glycerol in a 1:1 ratio. The resulting sample was loaded per well in the slot blot apparatus containing a nitrocellulose membrane under vacuum pressure. The membrane was blocked with a solution of 5% non-fat dried milk in TBS and incubated with the anti-HNE polyclonal antibody (1:200 dilution, Alpha Diagnostic, Vinci-Biochem, Vinci, Italy) overnight at 4 °C and 3 h at room temperature. An anti-rabbit IgG alkaline phosphatase secondary antibody (Dako, Glostrup, Denmark) was diluted 1:1500 in a solution of 5% non-fat dried milk in TBS and added to the membrane for 2 h at room temperature. Densitometric analysis was performed using Scion Image software. Data were normalized to α-tubulin.

2.9. Evaluation of ROS production in mitochondria

Mitochondrial ROS production was analyzed in real time by a video-rate confocal microscopy-based method. Briefly, cells were plated in glass wells and re-suspended after 24 h in a physiological buffer containing the ROS detection reagent (CM-H$_2$CFDA) at the final concentration of 1 μM. Cells were also loaded with Mitotracker Deep Red 633 FM (100 nM) (Invitrogen, Milan, Italy) for 45 min in 5% CO$_2$ at 37 °C for mitochondrial localization. CM-DCF fluorescence intensity was selectively recorded in mitochondria. Fluorescence emission intensity was calculated as the average green level value per pixel and corrected for background in at least 4 different fields.

2.10. Aβ aggregates production and cell treatment

The different aggregation states of Aβ$_{42}$ were obtained following the Dahlgren et al. protocol [27] with minor modifications. Briefly, lyophilized Aβ$_{42}$ peptides were dissolved in HFIP at a concentration of 1 mM. HFIP was removed by vacuum evaporation and the film was stored as aliquots in sterile microcentrifuge tubes at −80 °C until used. Immediately prior to the use, the film was solubilized in DMSO to a concentration of 5 mM. For oligomeric conditions, Ham's F12 was added to bring the peptide to

a final concentration of 100 μM and incubated at 4 °C for 6 days. For unaggregated conditions, the peptide was dissolved in DMSO and directly diluted into cell culture media. Oligomerization was monitored by western blotting using the mouse monoclonal antibody 6E10 (Santa Cruz Biotechnology, Inc. Heidelberg, Germany), specific for the residues 1–17 of Aβ, as previously described [28]. Then, cells were grown in 100-mm tissue culture dishes at an initial concentration of 2×10^6 cells/dish and were exposed to 1 μM of soluble and oligomeric forms of Aβ$_{42}$ for 6 and 24 h. Controls were performed in the presence of DMSO for each time point.

2.11. Measurements of proteasome activities in cell lysates

Proteasome peptidase activities in cell lysates were determined with fluorogenic peptides: Suc-Leu-Leu-Val-Tyr-AMC was used for ChT-L activity, Z-Leu-Ser-Thr-Arg-AMC for T-L activity, Z-Leu-Leu-Glu-AMC for PGPH activity, and Z-Gly-Pro-Ala-Phe-Gly-pAB for BrAAP activity [29]. The incubation mixture contained 1 μg of cell lysates, the appropriate substrate and 50 mM Tris–HCl pH 8.0, up to a final volume of 100 μL. Incubation was performed at 37 °C, and after 60 min the fluorescence of the hydrolyzed 7-amino-4-methyl-coumarin (AMC) and 4-aminobenzoic acid (pAB) was detected (AMC, $\lambda_{exc} = 365$ nm, $\lambda_{em} = 449$ nm; pAB, $\lambda_{exc} = 304$ nm, $\lambda_{em} = 664$ nm) on a SpectraMax Gemini XPS microplate reader. The 26S proteasome ChT-L activity was tested using Suc-Leu-Leu-Val-Tyr-AMC as substrate and 50 mM Tris–HCl pH 8.0 buffer containing 10 mM MgCl$_2$, 1 mM dithiothreitol, and 2 mM ATP. BrAAP activity was determined in a coupled test in the presence of aminopeptidase N. The effective 20S proteasome contribution to short peptide cleavage was evaluated with control experiments performed using specific proteasome inhibitors, Z-Gly-Pro-Phe-Leu-CHO and lactacystin (5 μM in the reaction mixture). The fluorescence values of lysates were subtracted of the values of control assays in the presence of the two inhibitors.

2.12. Measurements of cathepsins activities in cell lysates

Cathepsin B and L proteolytic activities were measured following the protocol described by Tchoupè et al. [30] using the fluorogenic peptides Z-Arg-Arg-AMC and Z-Phe-Arg-AFC. trifluoroacetate, respectively, at a final concentration of 50 μM. The mixture, containing 1 μg of protein lysate, was incubated in 100 mM phosphate buffer pH 6.0, 1 mM EDTA and 2 mM dithiothreitol for 1 h at 30 °C. The fluorescence of the hydrolyzed 7-amino-4-methyl-coumarin (AMC, $\lambda_{exc} = 365$ nm, $\lambda_{em} = 449$ nm) and 7-amino-4-trifluoromethylcoumarin (AFC, $\lambda_{exc} = 400$ nm, $\lambda_{em} = 505$ nm) was detected on a SpectraMax Gemini XPS microplate reader. The effective cathepsins contribution to the proteolysis was evaluated through control experiments performed using the specific inhibitors CA074Me and N-(1-naphthalenylsulfonyl)-Ile-Trp-aldehyde) for cathepsins B and L, respectively. Fluorescence values obtained by analyzing the lysates were then subtracted of the values of control assays in the presence of the two inhibitors.

2.13. Hsp90 immunoprecipitation

Hsp90 immunoprecipitation was conducted on cell lysates using an anti-Hsp90 antibody coupled with protein A-Sepharose CL-4B (Sigma-Aldrich, St Louis, MO, USA). The immunoprecipitation was carried out as previously described [31]. After immunoprecipitation, each pellet was resuspended in 50 μL Laemmli sample buffer, heated at 95 °C for 5 min, centrifuged for 30 s at 12,000×g, and pooled supernatants were used for western blotting analyses with an anti-acetylated lysine antibody (Santa Cruz Biotech., Heidelberg, Germany). Immunoblot detection with an anti-Hsp90-antibody (Santa Cruz Biotech., Heidelberg, Germany) was performed to verify the efficiency of the immunoprecipitation procedure and to control the equal protein loading.

2.14. Immunocytochemistry

For immunocytochemistry, cells were cultured in a Chamber Slide system, and after 24 h of incubation with both Aβ$_{42}$ forms, the monolayers were rapidly fixed in a 50:50 mixture of methanol and acetone for 5 min. For triple-labeling immunocytochemistry, monolayers were incubated first with the anti-20S core antibody (1:50, Enzo Life sciences, UK); with the anti-cathepsin B antibody (1:100, Santa Cruz Biotech., Heidelberg, Germany), and the anti-Aβ$_{42}$ antibody (1:50, JBC1766774, Millipore, Oak Drive, Temecula, CA), and then with biotin-labeled goat anti-rabbit (1:200, Jackson ImmunoResearch, West Grove, PA) secondary antibody. The binding of the antibody was detected with the Elite kit (Vector Laboratories), and the immunoreaction was developed using three different chromogens; violet (VIP, Vector, Burlingame UK) for cathepsin-B, grayish-black (diaminobenzidine hydrochloride developed with nickel addition, Vector) for anti-20S proteasome, and brown (DAB, Vector) for Aβ$_{42}$ stain. Lower-power digitized images were acquired with a BX-60 microscope (Olympus, Melville, NY) equipped with a DEI-470 digital camera (Optronics, Goleta, CA).

2.15. Statistical analysis

Results are expressed as mean values and standard deviation of results obtained from five separate experiments. Statistical analysis was performed with one way ANOVA, followed by the Bonferroni test using Sigma-stat 3.1 software (SPSS, Chicago, IL, USA). p-Values <0.05 and <0.01 were considered to be significant.

3. Results

### 3.1. Characterization of SH-SY5Y, APPwt and APPmut cells

3.1.1. Oxidative stress

Several clones of cells overexpressing wild type or mutant val717gly AβPP were developed. Cells were first characterized for AβPP overexpression. The two clones, stably transfected with either APPwt or APPmut, expressed comparable AβPP levels, but higher than those found in non-transfected cells (Fig. 1) and released significantly higher amounts of Aβ$_{42}$ (data not shown), as previously demonstrated by Zampagni et al. [32]. In detail, using the monoclonal antibody 6E10 that recognizes an epitope corresponding to the aa 1–17 inside the fragment Aβ$_{42}$ of the AβPP, we identified two bands, specifically the full length at 130 kDa and an isoform at 110 kDa (Fig. 1). It is in fact well demonstrated that AβPP exists in different isoforms and that its products can be also identified by western blotting analysis [33–37].

The two clones were compared in terms of redox profile by evaluating the levels of different oxidative markers, which are the final products of oxidation and nitrosylation processes. In particular, we focused on protein-bound HNE, which is one of the main products of lipid peroxidation [38], and on 3-NT and PC, established indicators of ROS-mediated protein oxidation [25,39,40]. Results are summarized in Table 1. Protein-bound HNE, 3-NT and PC levels were significantly higher in APPmut in comparison to APPwt cells. Moreover, all the three oxidative markers in APPwt were at least 2-folds higher that those found in SH-SY5Y non-transfected cells. As an additional index of cell redox state, we evaluated basal mitochondrial ROS levels using a confocal microscopy in living cells after exposure to the lowest laser light intensity (5%). Levels of mitochondrial ROS generated in APPmut were at least 3-folds higher compared to non-transfected cells. Surprisingly, APPwt mitochondria produced a very low amount of ROS in comparison with both APPmut and SH-SY5Y untransfected cells.

3.1.2. UPS and autophagy

Proteasomal and lysosomal activities were measured in the three cell lines as described in the Material and methods 2.11 and 2.12 sections and data are illustrated in Fig. 2. A different and subunit-dependent pattern of
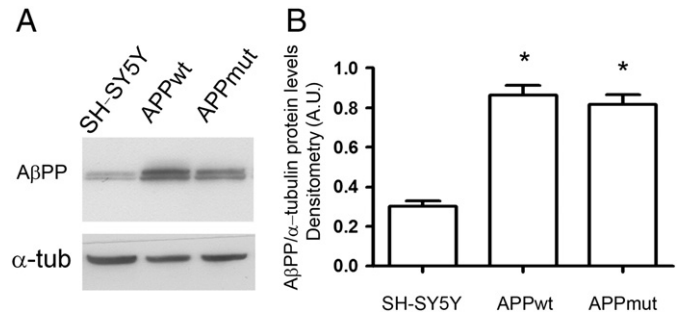
Fig. 1. AβPP levels in APPwt and APPmut cells. A) Representative western blotting of total extracts from SH-SY5Y neuroblastoma cells over-expressing wild-type AβPP gene (APPwt) or mutated AβPP gene (APPmut). Analysis was carried out using the monoclonal mouse 6E10 antibody. α-Tubulin was used as control for equal protein loading. B) Panel B shows the densitometric analysis of the AβPP amount performed in three different culture preparations of SH-SY5Y, APPwt and APPmut cell lines. Data points marked with an asterisk are statistically significant compared to control SH-SY5Y cells (*p<0.0002).

proteasome inhibition was observed in the two transfected cell lines (panel A). In details, in APPmut cells, except for the BrAAP, all the proteasomal components were severely compromised, whereas only the ChT-L activity was slightly reduced in APPwt cells. With respect to lysosomal proteolysis, both cathepsin B and L activities were markedly up-regulated in APPmut cells, whereas no differences were detected in APPwt cells compared to untransfected cells (panel B). Then, we monitored the state of the autophagic flux by stimulating autophagy through serum deprivation. Immunofluorescence analysis was performed to investigate the intracellular localization of the autophagosome membrane protein LC3. Two forms of LC3, namely LC3-I (cytosolic) and LC3-II (membrane-bound), were produced post-translationally in various cells. During the activation of autophagy, LC3-I is processed and recruited to autophagosome, where LC3-II is generated by site-specific proteolysis and lipidation near the C-terminus. Fig. 3 shows the immunofluorescence analysis carried out with an anti-LC3 antibody, which recognizes the two isoforms. In SH-SY5Y untransfected cells, LC3 immunostaining was diffuse, indicative of the more abundant cytoplasmic isoform LC3-I. When cells were starved, LC3 peculiar punctuate staining was observed, pinpointing the autophagosome formation. Interestingly, SH-SY5Y cells stably transfected with wild-type APP yet in basal condition expressed the LC3 punctuate staining, suggesting an autophagic process in place. After 8 h of starvation, cells appeared similar to the basal condition control, suggesting that the serum deprivation stimulus did not activate the autophagy process in APPwt clone. Also in APPmut cells after the starvation stimulus, only very limited LC3 immunopositive dots were observed, but, different from the wild type counterpart, cells overexpressing AβPP mutant in basal condition showed a diffuse staining with anti-LC3 antibody (Fig. 3, panel A).

The levels of the autophagy related proteins LC3-II, beclin-1 and p62 and of Ub–protein conjugates were detected through western blotting assays. While beclin-1 plays a key role in autophagy being involved in

Table 1
Oxidative profile in SH-SY5Y overexpressing APPwt and APPmut. Oxidative stress was evaluated as the expression of HNE-Michael adducts, 3-nitro-tyrosine (3-NT) and protein carbonyl (PC) levels, as well as the amount of ROS inside the mitochondria.

	HNE-Michael adducts	3-NT	PC	Mitochondrial ROS
SH-SY5Y	1.2 ± 0.18	0.62 ± 0.16	0.85 ± 0.17	187.00 ± 38.01
APPwt	2.90 ± 0.75	1.61 ± 0.18	1.95 ± 0.56	98.86 ± 29.67
APPmut	4.30 ± 0.95*	2.78 ± 0.08**	2.80 ± 0.38***	453.33 ± 32.51§

*p<0.001 APPmut vs SH-SY5Y; **p<0.005 APPmut vs SH-SY5Y; ***p<0.005 APPmut vs SH-SY5Y; §p<0.005 APPmut vs SH-SY5Y.
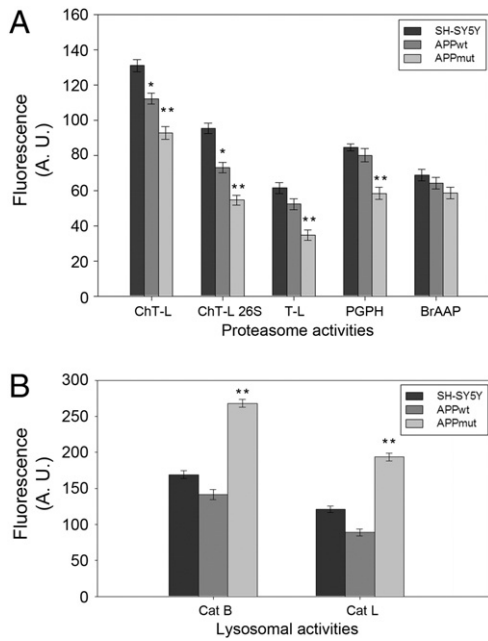
Fig. 2. Basal activity of the UPS and cathepsins in SH-SY5Y, APPwt and APPmut cells. Cells were investigated for the basal activity of both the UPS (panel A) and cathepsins (panel B). Results are presented as fluorescence units. Data points marked with an asterisk are statistically significant compared to control SH-SY5Y cells (*p<0.05, **p<0.01).

the enrolment of membranes to form autophagosomes, p62 binds to both LC3-II and ubiquitin, and is finally degraded in autophagolysosomes [41,42]. Therefore, its levels inversely correlate with the autophagic activity. Data are illustrated in Fig. 3 (panels C and D). In accordance with the immunofluorescence data, serum starved APPmut cells displayed a defect in the autophagosome formation process, showing lower levels of both LC3-II and beclin-1 compared to control SH-SY5Y cells. Conversely, the amount of both proteins did not change in APPwt cells, confirming the absence of autophagy activation upon the starvation stimulus. As for p62, in line with previous data demonstrating significantly lower p62 cytosolic levels in the frontal cortex of AD patients compared to control subjects [43], we observed lower basal amounts in APPmut cells compared to untransfected SH-SY5Y cells. When cells were starved, in both cell lines a decrease in p62 levels was detected, indicative of no changes at this phase of the autophagic cascade. Finally, serum deprivation promoted the accumulation of Ub–protein conjugates, most likely in response to the production of ROS associated to the serum deficiency [44,45].

In this scenario, with the overexpression of the amyloid precursor protein determining an extensive re-modulation of the interplay between proteasome and autophagy in neurons, we tried to individuate a possible intermediary in such reorganization focusing our attention on the histone deacetylase 6 (HDAC6). Analyzing our models, we obtained higher expression levels and an enhanced HDAC6 activity, measured in terms of Hsp90-lysine acetylation, in APPmut cells (Figs. 4–9), suggesting the cellular attempt to activate compensatory autophagy in response to the severe proteasomal inhibition.
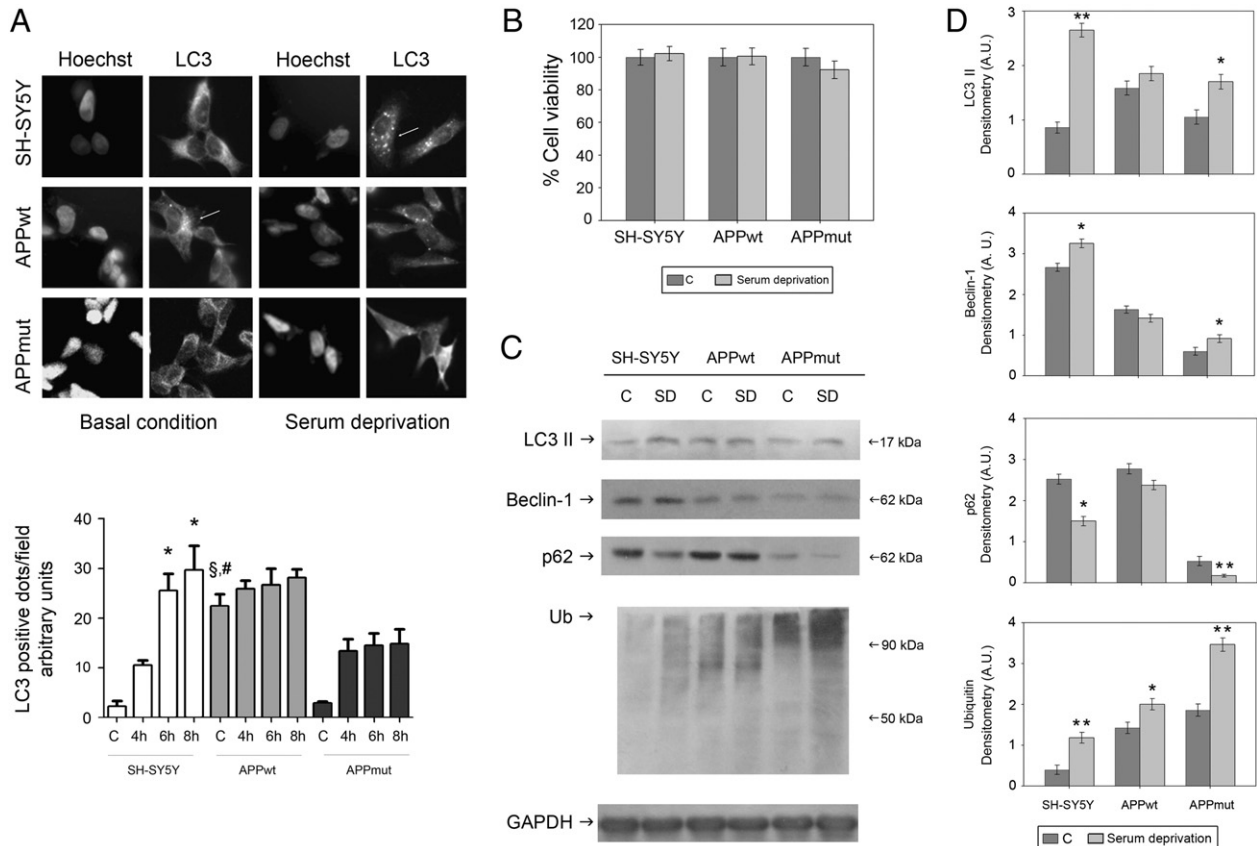
Fig. 3. Detection of autophagy-related proteins. Panel A. LC3 fluorescent identification and Hoechst stain in SH-SY5Y, APPwt and APPmut cells in basal condition and upon serum deprivation. *p<0.0001 SH-SY5Y at 6 h and SH-SY5Y at 8 h vs SH-SY5Y cont, §p<0.0001 APPwt vs SH-SY5Y control, #p<0.0001 APPwt vs APPmut cells. Then, cells were serum starved for 8 h and cell viability was determined with the MTT assay (panel B). Lysates were analyzed for autophagy-related proteins (LC3-II, beclin-1 and p62) and Ub–protein conjugates. Panels C and D show respectively representative immunoblots and densitometric analyses obtained from five separate experiments. Equal protein loading was verified by using an anti-GAPDH antibody. The detection was executed by an ECL western blotting analysis system. Data points marked with an asterisk are statistically significant compared to their respective non treated control cells (*p<0.05, **p<0.01). (A.U.) arbitrary units.
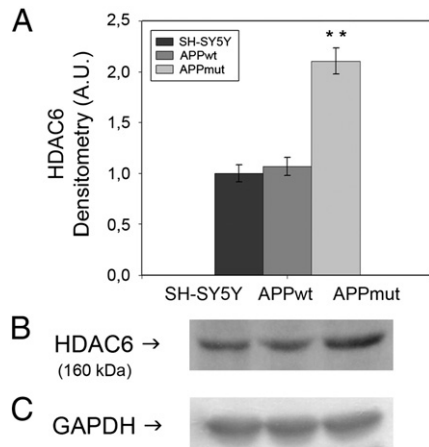
Fig. 4. Detection of HDAC6 levels. HDAC6 expression in control SH-SY5Y, APPwt and APPmut cells. Panel A shows the densitometric analysis obtained from five separate blots and panel B shows a representative immunoblot. Equal protein loading was verified by using an anti-GAPDH antibody (panel C). The detection was executed by an ECL western blotting analysis system. Data points marked with an asterisk are statistically significant compared to their respective non treated control cells (*p<0.05, **p<0.01). (A.U.) arbitrary units.

3.2. Cellular localization of the 20S proteasome, cathepsin B and $A\beta_{42}$

Upon 24 h of amyloid treatment, cells were assayed for the simultaneous detection of the 20S proteasome, the $A\beta_{42}$ and the cathepsin B. Pictures were obtained after trichrome staining with the three antibodies. The proteasome is colored in black, the $A\beta_{42}$ in brown and the cathepsin B in purple (Fig. 5). SH-SY5Y cells showed an evident nuclear expression of the 20S proteasome particularly marked upon oligomer treatment. Furthermore, when cells were exposed to the soluble form of the peptide we obtained the co-expression of the cathepsin B and the 20S core, with higher levels of the lysosomal enzyme with respect to the proteasome. High expression levels of the 20S proteasome were

detected in the APPwt cells exposed to amyloid oligomers. APPmut cells displayed a very singular pattern. When these cells were treated with the soluble form of the peptide, they displayed a marked expression of the cathepsin B with almost no signal for the 20S proteasome. The detection of the 20S core was more evident upon treatment with oligomers. Interestingly, both APPwt and APPmut clones displayed an evident cathepsin B nuclear expression, indicating the contribution of the enzyme to nuclear alterations occurring in AD.

### 3.3. Proteasome activities in amyloid treated cells

Cells were treated with 1 μM of $A\beta_{42}$ in its soluble and oligomeric forms. No significant change in cell survival was observed, just a 15% decrease after 24 h of treatment with amyloid oligomeric species. Furthermore, the three cell lines did not show morphological differences in response to the treatment (data not shown). Following amyloid exposure, proteasome activities on cell lysates were measured. Results related to the four 20S proteasome components and to the ChT-L activity of the 26S proteasome are illustrated in Fig. 6. Data indicate a significant inhibition of the enzymatic complex with a marked decrease of all the tested activities, particularly evident upon 24 h of treatment and in the presence of $A\beta_{42}$ oligomers. APPmut cells were the most susceptible to the treatment. Western blotting assays with anti-20S proteasome antibodies did not show any changes in 20S core expression upon amyloid treatment, demonstrating that the decrease in proteasome functionality was effectively related to a reduced activity rather than to a lower expression of its subunits (data not shown). Such data were also confirmed by the accumulation of Ub-conjugates, known markers of proteasome inhibition, mainly in response to a 24 h treatment with oligomeric structures (Fig. 7).

3.4. Cathepsins activities in amyloid treated cells

Cathepsins are proteolytic enzymes responsible for the endosomal–lysosomal degradation. We monitored the lysosomal functionality measuring the activity of cathepsins B and L that were demonstrated to play
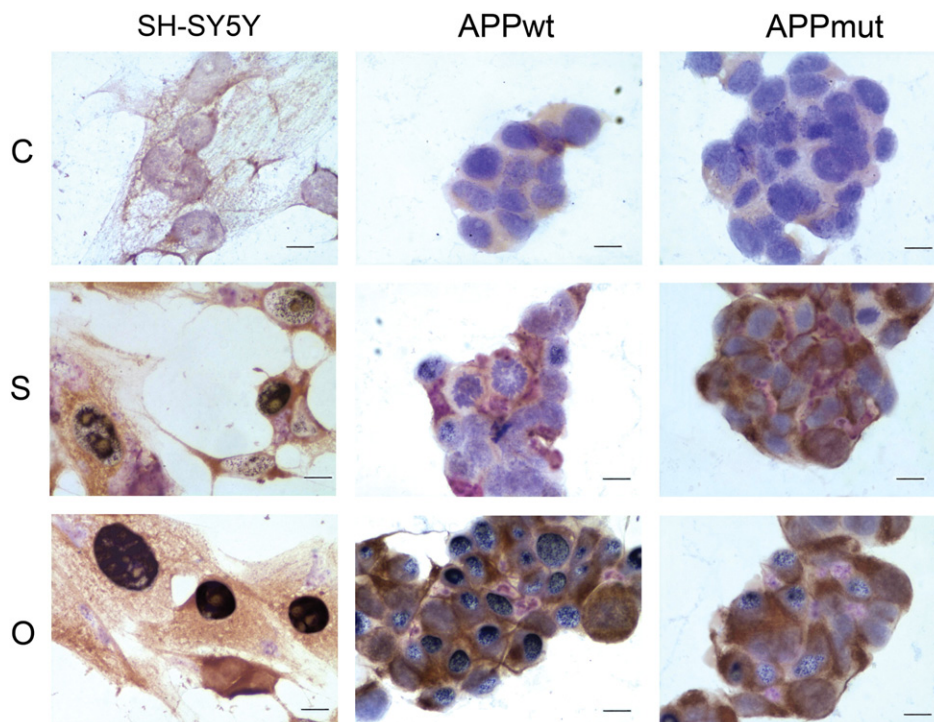
Fig. 5. 20S proteasome, $A\beta_{42}$ and cathepsin B cellular localization. Upon 24 h of exposure to 1 μM $A\beta_{42}$ soluble (S) and oligomeric forms (O), control SH-SY5Y, APPwt and APPmut cells were analyzed for the localization of cathepsin B (violet), $A\beta_{42}$ (brown) and 20S core (black). (C): non treated control cells. Scale bar 50 μm.
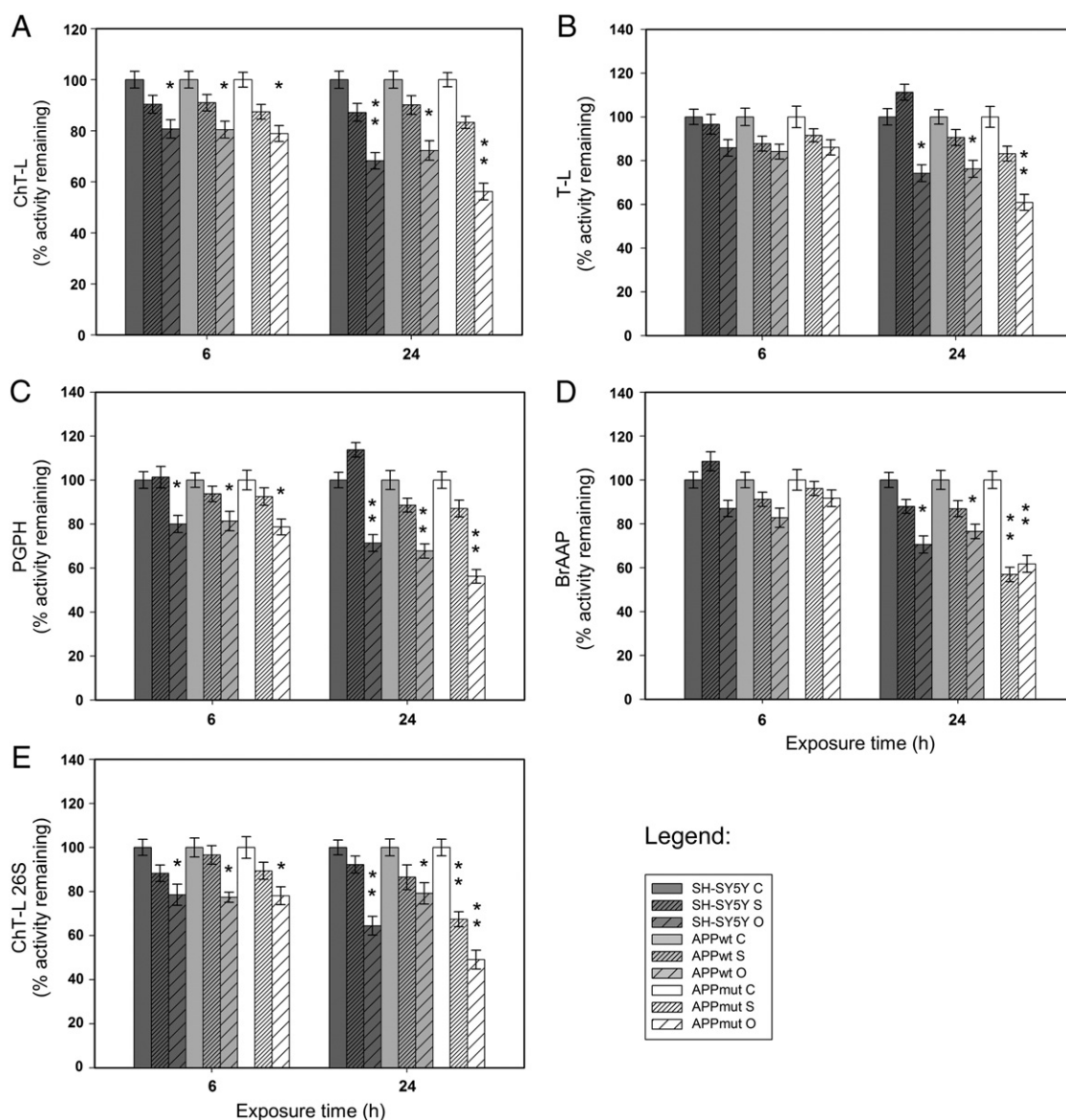
Fig. 6. Effect of Aβ$_{42}$ treatment on UPS activity. Proteasome activities were measured in cell lysates upon 6 and 24 h of exposure to 1 μM of soluble and oligomeric forms of Aβ$_{42}$ as described in the Material and methods 2.11 section. (C) Control, (S) Aβ$_{42}$ soluble forms and (O) Aβ$_{42}$ oligomers. Results are presented as percentage of activity remaining toward control in each time set. Fluorescence units were subtracted of the values of control assays in the presence of specific inhibitors. Data points marked with an asterisk are statistically significant compared to their respective non treated control cells ($^*p<0.05$, $^{**}p<0.01$).

a role in the AβPP processing [12]. After amyloid treatment, only the APPmut cell line showed an impaired enzymatic activity. Interestingly, the inhibition was already evident upon short exposure time (6 h) (Fig. 8). Western blotting assays using anti-cathepsin B and anti-cathepsin L antibodies confirmed that such inhibition was not the consequence of a decreased expression of the cathepsins (data not shown).

3.5. Expression of HDAC6 and Hsp90 acetylation in amyloid treated cells

HDAC6 is considered an important link between UPS and autophagy. Previously, we indicated that APPmut cells were characterized by high levels of HDAC6 and by a parallel decrease of the Hsp90 acetylated lysine content. Upon cell treatment with the amyloid peptide increased levels of this deacetylase were detected (Fig. 9, left panel). Such amplified expression was mainly evident in the APPmut cell line. In fact, the exposure to oligomeric structures and to the soluble form of the protein

caused HDAC6 levels 1.54- and 1.17-fold higher, respectively, compared to control untreated cells. To gain further insight into the regulation of the intracellular proteolysis upon amyloid treatment, we measured the activity of HDAC6 in terms of Hsp90 lysine acetylation (Fig. 9, right panel). Consistent with the increased levels of HDAC6, the immunoprecipitated Hsp90 showed a decrease in its extent of acetylation. In detail, considering the APPmut cell line, the treatment with the soluble peptide and with the oligomers caused a 1.82- and 2.20-fold decrease, respectively, compared to control APPmut untreated cells.

4. Discussion

The UPS and autophagy have been thought as relatively distinct systems sharing a common role and a common substrate: the proteolysis of misfolded proteins. However, recent findings strongly suggest the existence of a crosstalk and even a cooperation between these two degradation pathways [46]. Both systems are involved in the onset of
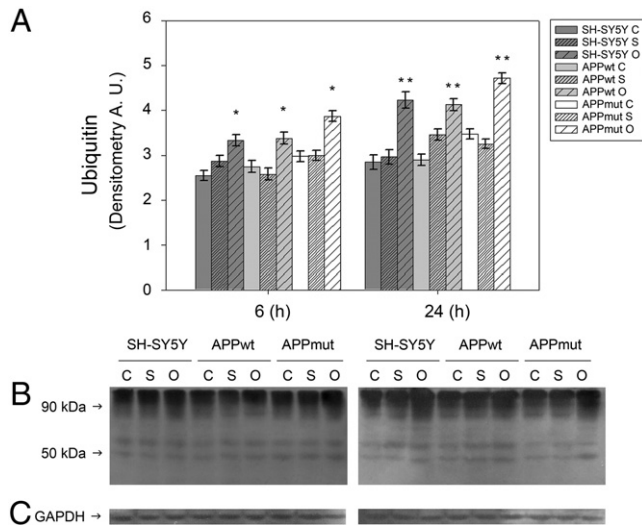
Fig. 7. Effect of Aβ$_{42}$ treatment on Ub–protein conjugates. Levels of Ub–protein conjugates in SH-SY5Y, APPwt and APPmut cells treated with Aβ$_{42}$ for 6 and 24 h. (C) Control, (S) Aβ$_{42}$ soluble forms and (O) Aβ$_{42}$ oligomers. Panel A shows the densitometric analysis obtained from five separate blots and panel B shows a representative immunoblot. Equal protein loading was verified by using an anti-GAPDH antibody (panel C). The detection was executed by an ECL Western Blotting analysis system. Data points marked with an asterisk are statistically significant compared to their respective not treated control cells (p<0.05, **p<0.01). (A.U.) arbitrary units.

neurodegenerative disorders and failures in their activities promote neuronal death mechanisms. In the present study, we analyzed the relationship between the UPS and autophagy in a human cellular model of AD, investigating how proteolysis was regulated in such a compromised condition. Specifically, the study was carried out on SH-SY5Y neuroblastoma cells stably transfected with wild-type AβPP gene (APPwt) or 717 valine-to-glycine AβPP-mutated gene (APPmut). The two clones

expressed a comparable amount of AβPP protein, although the APPmut clone produced and released significantly higher amounts of Aβ$_{42}$ as previously described by Zampagni et al. [32]. The analysis of oxidative markers, such as the HNE Michael adduct, 3-NT and PC levels, provided evidence that AβPP over-expression and Aβ$_{42}$ overload induced oxidative stress and increased the vulnerability to oxidative stress, contributing significantly to neuronal death in AD. Nevertheless, oxidative markers were significantly higher in APPmut cells than those found in the APPwt clone, suggesting the direct correlation between Aβ$_{42}$ levels and oxidative stress, in agreement with previous studies [47,48]. Data on mitochondrial ROS generation showed that differences between APPmut and APPwt clones were not only in terms of oxidative stress amount, but probably they developed a different strategy to compensate for the detrimental environment. In fact, it is noteworthy that the APPwt clone expressed very low levels of ROS inside the mitochondria, whereas ROS production was very high in APPmut cells. At this regard, Cenini et al. [49] demonstrated in HEK293 cells stably transfected with APP751wt the presence of adaptive responses, including an increased expression and activity of Mn-superoxide dismutase, to counteract an increased oxidative stress. However, in HEK-APP751 717 valine-to-glycine mutant clone, oxidative stress was so high that cells were not able to develop such strategies. This behavior observed in HEK APPwt as well as in SH-SY5Y APPwt is explained by the "hormesis theory" [50,51]. The fact that a strong increase in oxidative stress and an impaired mitochondrial functionality always accompany AD makes them an appealing target for possible therapeutic interventions. Besides the conventional antioxidant-based therapies, alternative strategies, such as the possibility to potentiate cellular stress responses through hormetic stimulation, are under investigation. At this regard, a promising target could be represented by vitagenes, a class of sensitive and cytoprotective genes involved in preserving cellular homeostasis during stressful conditions [52,53]. Among vitagene products, molecules endowed with antioxidant and anti-apoptotic activities (heat shock proteins Hsp32, Hsp70, glutathione, the thioredoxin and the sirtuin protein systems) are included. This network acts in response to age-associated mitochondrial dysfunctions and is modulated
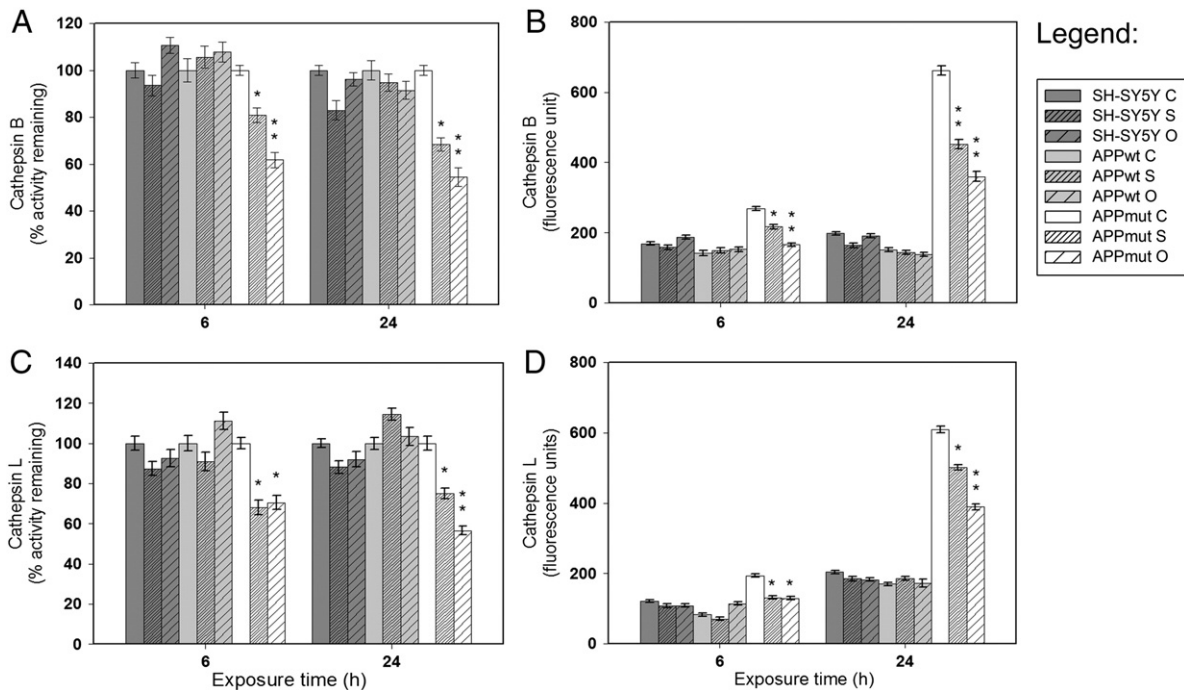
Fig. 8. Effect of Aβ$_{42}$ treatment on cathepsin B and L activity. Activities of both cathepsin B and cathepsin L were measured in cell lysates upon 6 and 24 h of exposure to 1 μM of soluble and oligomeric forms of Aβ$_{42}$ as described in the Material and Methods 2.11 section. (C) Control, (S) Aβ$_{42}$ soluble forms and (O) Aβ$_{42}$ oligomers. Results are presented both as percentage of activity remaining toward non treated control cells (A–C) and as fluorescence units (B–D). Data were subtracted of the values of control assays in the presence of specific inhibitors. Data points marked with an asterisk are statistically significant compared to their respective non treated control cells (*p<0.05, **p<0.01).
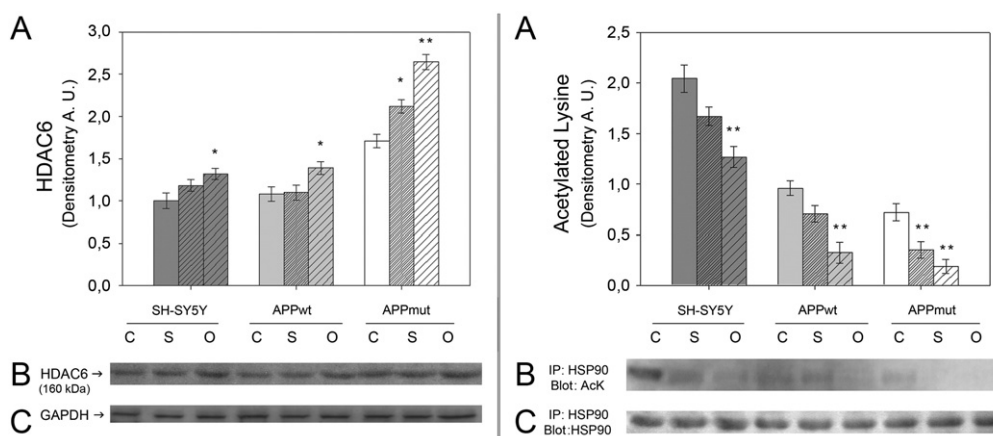
Fig. 9. Effect of Aβ_{42} treatment on HDAC6 levels and activity. Left box: HDAC6 levels in SH-SY5Y, APPwt and APPmut cells treated with Aβ_{42} for 24 h. Panel A shows the densitometric analysis obtained from five separate blots and panel B shows a representative western blotting. Equal protein loading was verified by using an anti-GAPDH antibody (panel C). Right box: HDAC6 activity was measured in terms of Hsp90 acetylation. SH-SY5Y, APPwt and APPmut cells were treated with Aβ_{42} for 24 h. Cell lysates were then immunoprecipitated with an anti-Hsp90 antibody followed by immunoblotting with an anti-Ack antibody. Panel A shows the densitometric analysis obtained from five separate blots and panel B shows a representative immunoblot. The equal amount of immunoprecipitated Hsp90 was verified using anti-Hsp90 antibody (panel C). (C): Control, (S): Aβ_{42} soluble forms, (O): Aβ_{42} oligomers. The detection was executed by an ECL analysis system. Data points marked with an asterisk are statistically significant compared to their respective non treated control cells (*$p < 0.05$, **$p < 0.01$). (A.U.) arbitrary units.

by mitochondrial free radicals [54]. As suggested by Calabrese et al., a deeper understanding of the relationship between the vitagene network and the hormetic dose response mechanisms may support the stimulation of maintenance and repair pathways through exogenous interventions, such as mild stress or nutritional antioxidants targeting the vitagene network, as a novel approach for those pathophysiological conditions, including neurodegenerative disorders [53–55].

The elevated levels of Aβ_{42} and the increased oxidative damage observed in APPmut cells determined a significantly altered proteolytic pattern with the inhibition of the proteasome functionality and the deregulation of the autophagic pathway. This latter was confirmed by the increase in cathepsins activity and by the parallel defects in autophagosome formation. Additionally, both clones displayed a marked nuclear staining of cathepsin B, suggesting that lysosomal enzymes participate to the nuclear alterations occurring in AD [56]. Previous data reported on the ability of the cytoplasmic enzyme HDAC6 to mediate the compensatory activation of autophagy in *D. melanogaster* models of spinobulbar muscular atrophy [15,19]. Based on these observations, we focused our attention on this deacetylase as a possible intermediary of the observed proteolysis re-modulation. Interestingly, our results showed that APPmut cells displayed higher expression levels and an enhanced activity of HDAC6, supporting the hypothesis that in AD pathogenesis cells try to remedy to proteasomal inhibition by activating HDAC6-dependent autophagy.

A similar approach to clarify the molecular mechanism underlying Aβ neurotoxicity was followed by Matsumoto et al. who found in SH-SY5Y cells overexpressing AβPP a reduced proteasomal activity associated to increased susceptibility to oxidative stress. However, in this work such alterations were observed upon the APPwt overexpression whereas the expression of APPmut (His684Arg mutation) increased Aβ_{42} excretion, but did not affect cell properties [57].

Cells were then treated with Aβ_{42}, the most toxic amyloid beta form, to better elucidate its contribution to the different phenotypes observed in our models. We already demonstrated that SH-SY5Y cells treated with amyloid oligomers showed a compromised proteasome activity [28]. In the present work we provided evidence that, upon amyloid treatment, the proteasomal functionality resulted clearly impaired not only in APPmut cells but also in APPwt clones and control SH-SY5Y cells, suggesting the existence of a critical Aβ_{42} threshold beyond which the proteasomal machinery becomes dysfunctional. Such alterations were considerably visible after exposure to Aβ_{42} oligomers and matched with the accumulation of Ub-conjugates. In addition, the nuclear redistribution and accumulation of 20S proteasome upon oligomer exposure

suggested that the proteasome takes part in DNA repair and/or cell death mechanisms occurring in AD.

Upon amyloid treatment, the previously reported upregulation of HDAC6 was now evident in all the analyzed models, both in terms of expression and activity, indicative of the cellular attempt to trigger the autophagic pathway in response to oligomer-associated proteasome impairment. Interestingly, the increased HDAC6 activity induced an almost complete deacetylation of its substrate Hsp90, which in the hypoacetylated form is able to carry out its normal role.

Control SH-SY5Y and APPwt cells did not show alterations in cathepsins B and L activities in response to the amyloid treatment whereas inhibited functionalities were observed in APPmut clones. Aβ_{42} aggregates were demonstrated to induce pro-oxidative effects to the lysosomal membrane in SH-SY5Y cells with the loss of impermeability and leakage of lysosomal hydrolases into the cytosol [58,59]. Here we propose that the increase in Aβ_{42} content and elevated levels of oxidative damage in APPmut cells contribute to lysosomal membrane alterations. As neurons become more compromised by the excess in amyloid content, the initial lysosomal system up-regulation observed in non-treated APPmut cells is replaced by lysosomal dysfunctions. In addition, previous studies illustrated that Aβ_{42} is selectively uptaken by neurons and that the peptide is extremely resistant to degradation, favoring the accumulation of the protein and the increase of C-terminal APP fragments, which in turn further promote the production of Aβ_{42} [60,61]. According to these data, it is reasonable to hypothesize that in our models the internalized amyloid stimulates such mechanisms and contributes to the generation of new toxic amyloid species. Finally, the amyloid peptide overload induces the dramatic inhibition of both the proteasome and cathepsins activities, leading to neuronal degeneration.

Concluding, our findings indicate that the excessive release of Aβ_{42} promotes a remarkable reorganization of the crosstalk between UPS and autophagy and demonstrate the existence of an amyloid threshold beyond which cellular proteolysis becomes definitely dysfunctional. However, more efforts are needed to explore the functional relationship between the UPS and autophagy and to widen our knowledge of the mechanisms through which misfolded proteins are oriented toward one proteolytic system or the other.

Acknowledgements

References

[1] D.J. Selkoe, Alzheimer's disease: genes, proteins, and therapy, Physiol. Rev. 81 (2001) 741–766.

[2] A. Rocchi, S. Pellegrini, G. Siciliano, L. Murri, Causative and susceptibility genes for Alzheimer's disease: a review, Brain Res. Bull. 61 (2003) 1–24.

[3] F. Flood, S. Murphy, R.F. Cowburn, L. Lannfelt, B. Walker, J.A. Johnston, Proteasome-mediated effects on amyloid precursor protein processing at the gamma-secretase site, Biochem. J. 385 (2005) 545–550.

[4] P. Kienlen-Campard, C. Feyt, S. Huysseune, P. de Diesbach, F. N'Kuli, P.J. Courtoy, J.N. Octave, Lactacystin decreases amyloid-beta peptide production by inhibiting beta-secretase activity, J. Neurosci. Res. 84 (2006) 1311–1322.

[5] M. Orlowski, S. Wilk, Catalytic activities of the 20 S proteasome, a multicatalytic proteinase complex, Arch. Biochem. Biophys. 383 (2000) 1–16.

[6] P. Deriziotis, S.J. Tabrizi, Prions and the proteasome, Biochim. Biophys. Acta 1782 (2008) 713–722.

[7] V. Cecarini, Q. Ding, J.N. Keller, Oxidative inactivation of the proteasome in Alzheimer's disease, Free. Radic. Res. 41 (2007) 673–680.

[8] J.N. Keller, K.B. Hanni, W.R. Markesbery, Impaired proteasome function in Alzheimer's disease, J. Neurochem. 75 (2000) 436–439.

[9] F. Checler, C.A. da Costa, K. Ancolio, N. Chevallier, E. Lopez-Perez, P. Marambaud, Role of the proteasome in Alzheimer's disease, Biochim. Biophys. Acta 1502 (2000) 133–138.

[10] V. Kaminskyy, B. Zhivotovsky, Proteases in autophagy, Biochim. Biophys. Acta 1824 (2012) 44–50.

[11] E. Wong, A.M. Cuervo, Autophagy gone awry in neurodegenerative diseases, Nat. Neurosci. 13 (2010) 805–811.

[12] D.M. Klein, K.M. Felsenstein, D.E. Brenneman, Cathepsins B and L differentially regulate amyloid precursor protein processing, J. Pharmacol. Exp. Ther. 328 (2009) 813–821.

[13] V.Y. Hook, M. Kindy, G. Hook, Inhibitors of cathepsin B improve memory and reduce beta-amyloid in transgenic Alzheimer disease mice expressing the wild-type, but not the Swedish mutant, beta-secretase site of the amyloid precursor protein, J. Biol. Chem. 283 (2008) 7745–7753.

[14] N.A. Kaniuk, M. Kiraly, H. Bates, M. Vranic, A. Volchuk, J.H. Brumell, Ubiquitinated–protein aggregates form in pancreatic beta-cells during diabetes-induced oxidative stress and are regulated by autophagy, Diabetes 56 (2007) 930–939.

[15] U.B. Pandey, Z. Nie, Y. Batlevi, B.A. McCray, G.P. Ritson, N.B. Nedelsky, S.L. Schwartz, N.A. DiProspero, M.A. Knight, O. Schuldiner, R. Padmanabhan, M. Hild, D.L. Berry, D. Garza, C.C. Hubbert, T.P. Yao, E.H. Baehrecke, J.P. Taylor, HDAC6 rescues neurodegeneration and provides an essential link between autophagy and the UPS, Nature 447 (2007) 859–863.

[16] Y. Kawaguchi, J.J. Kovacs, A. McLaurin, J.M. Vance, A. Ito, T.P. Yao, The deacetylase HDAC6 regulates aggresome formation and cell viability in response to misfolded protein stress, Cell 115 (2003) 727–738.

[17] J.Y. Lee, H. Koga, Y. Kawaguchi, W. Tang, E. Wong, Y.S. Gao, U.B. Pandey, S. Kaushik, E. Tresse, J. Lu, J.P. Taylor, A.M. Cuervo, T.P. Yao, HDAC6 controls autophagosome maturation essential for ubiquitin-selective quality-control autophagy, EMBO J. 29 (2010) 969–980.

[18] J.J. Kovacs, P.J. Murphy, S. Gaillard, X. Zhao, J.T. Wu, C.V. Nicchitta, M. Yoshida, D.O. Toft, W.B. Pratt, T.P. Yao, HDAC6 regulates Hsp90 acetylation and chaperone-dependent activation of glucocorticoid receptor, Mol. Cell. 18 (2005) 601–607.

[19] U.B. Pandey, Y. Batlevi, E.H. Baehrecke, J.P. Taylor, HDAC6 at the intersection of autophagy, the ubiquitin–proteasome system and neurodegeneration, Autophagy 3 (2007) 643–645.

[20] M. Orlowski, C. Michaud, Pituitary multicatalytic proteinase complex. Specificity of components and aspects of proteolytic activity, Biochemistry 28 (1989) 9270–9278.

[21] G. Pfleiderer, Isolation of an aminopeptidase from kidney particles, in: G.E. Perlman, L. Lorand (Eds.), Methods in Enzymology, Academic Press, New York, NY, 1970.

[22] M.M. Bradford, A rapid and sensitive method for the quantitation of microgram quantities of protein utilizing the principle of protein-dye binding, Anal. Biochem. 72 (1976) 248–254.

[23] C. Marchini, M. Angeletti, A.M. Eleuteri, A. Fedeli, E. Fioretti, Aspirin modulates LPS-induced nitric oxide release in rat glial cells, Neurosci. Lett. 381 (2005) 86–91.

[24] T. Mosmann, Rapid colorimetric assay for cellular growth and survival: application to proliferation and cytotoxicity assays, J. Immunol. Methods 65 (1983) 55–63.

[25] D.A. Butterfield, E.R. Stadtman, Protein oxidation processes in aging brain, Adv. Cell Aging Gerontol. 2 (1997) 161–191.

[26] J. Drake, R. Sultana, M. Aksenova, V. Calabrese, D.A. Butterfield, Elevation of mitochondrial glutathione by gamma-glutamylcysteine ethyl ester protects mitochondria against peroxynitrite-induced oxidative stress, J. Neurosci. Res. 74 (2003) 917–927.

[27] K.N. Dahlgren, A.M. Manelli, W.B. Stine Jr., L.K. Baker, G.A. Krafft, M.J. LaDu, Oligomeric and fibrillar species of amyloid-beta peptides differentially affect neuronal viability, J. Biol. Chem. 277 (2002) 32046–32053.

[28] V. Cecarini, L. Bonfili, M. Amici, M. Angeletti, J.N. Keller, A.M. Eleuteri, Amyloid peptides in different assembly states and related effects on isolated and cellular proteasomes, Brain Res. 1209 (2008) 8–18.

[29] A.M. Eleuteri, M. Angeletti, G. Lupidi, R. Tacconi, L. Bini, E. Fioretti, Isolation and characterization of bovine thymus multicatalytic proteinase complex, Protein Expr. Purif. 18 (2000) 160–168.

[30] J.R. Tchoupe, T. Moreau, F. Gauthier, J.G. Bieth, Photometric or fluorometric assay of cathepsin B, L and H and papain using substrates with an aminotrifluoromethylcoumarin leaving group, Biochim. Biophys. Acta 1076 (1991) 149–151.

[31] M. Amici, V. Cecarini, M. Cuccioloni, M. Angeletti, S. Barocci, G. Rossi, E. Fioretti, J.N. Keller, A.M. Eleuteri, Interplay between 20S proteasomes and prion proteins in scrapie disease, J. Neurosci. Res. 88 (2010) 191–201.

[32] M. Zampagni, E. Evangelisti, R. Cascella, G. Liguri, M. Becatti, A. Pensalfini, D. Uberti, G. Cenini, M. Memo, S. Bagnoli, B. Nacmias, S. Sorbi, C. Cecchi, Lipid rafts are primary mediators of amyloid oxidative attack on plasma membrane, J. Mol. Med. (Berl.) 88 (2010) 597–608.

[33] S. Eggert, K. Paliga, P. Soba, G. Evin, C.L. Masters, A. Weidemann, K. Beyreuther, The proteolytic processing of the amyloid precursor protein gene family members APLP-1 and APLP-2 involves alpha-, beta-, gamma-, and epsilon-like cleavages: modulation of APLP-1 processing by n-glycosylation, J. Biol. Chem. 279 (2004) 18146–18156.

[34] C. Galli, A. Piccini, M.T. Ciotti, L. Castellani, P. Calissano, D. Zaccheo, M. Tabaton, Increased amyloidogenic secretion in cerebellar granule cells undergoing apoptosis, Proc. Natl. Acad. Sci. U. S. A. 95 (1998) 1247–1252.

[35] M.G. Schlossmacher, B.L. Ostaszewski, L.I. Hecker, A. Celi, C. Haass, D. Chin, I. Lieberburg, B.C. Furie, B. Furie, D.J. Selkoe, Detection of distinct isoform patterns of the beta-amyloid precursor protein in human platelets and lymphocytes, Neurobiol. Aging 13 (1992) 421–434.

[36] D.J. Selkoe, M.B. Podlisny, C.L. Joachim, E.A. Vickers, G. Lee, L.C. Fritz, T. Oltersdorf, Beta-amyloid precursor protein of Alzheimer disease occurs as 110- to 135-kilodalton membrane-associated proteins in neural and nonneural tissues, Proc. Natl. Acad. Sci. U. S. A. 85 (1988) 7341–7345.

[37] P.R. Turner, K. O'Connor, W.P. Tate, W.C. Abraham, Roles of amyloid precursor protein and its fragments in regulating neural activity, plasticity and memory, Prog. Neurobiol. 70 (2003) 1–32.

[38] D.A. Butterfield, C.M. Lauderback, Lipid peroxidation and protein oxidation in Alzheimer's disease brain: potential causes and consequences involving amyloid beta-peptide-associated free radical oxidative stress, Free Radic. Biol. Med. 32 (2002) 1050–1060.

[39] A. Castegna, V. Thongboonkerd, J.B. Klein, B. Lynn, W.R. Markesbery, D.A. Butterfield, Proteomic identification of nitrated proteins in Alzheimer's disease brain, J. Neurochem. 85 (2003) 1394–1401.

[40] R. Sultana, S.F. Newman, Q. Huang, D. Allan Butterfield, Detection of carbonylated proteins in two-dimensional sodium dodecyl sulfate polyacrylamide gel electrophoresis separations, Methods Mol. Biol. 476 (2009) 149–159.

[41] Y. Cao, D.J. Klionsky, Physiological functions of Atg6/Beclin 1: a unique autophagy-related protein, Cell Res. 17 (2007) 839–849.

[42] G. Bjorkoy, T. Lamark, S. Pankiv, A. Overvatn, A. Brech, T. Johansen, Monitoring autophagic degradation of p62/SQSTM1, Methods Enzymol. 452 (2009) 181–197.

[43] Y. Du, M.C. Wooten, M. Gearing, M.W. Wooten, Age-associated oxidative damage to the p62 promoter: implications for Alzheimer disease, Free Radic. Biol. Med. 46 (2009) 492–501.

[44] S.I. Kang, H.W. Choi, I.Y. Kim, Redox-mediated modification of PLZF by SUMO-1 and ubiquitin, Biochem. Biophys. Res. Commun. 369 (2008) 1209–1214.

[45] S. Pandey, C. Lopez, A. Jammu, Oxidative stress and activation of proteasome protease during serum deprivation-induced apoptosis in rat hepatoma cells; inhibition of cell death by melatonin, Apoptosis 8 (2003) 497–508.

[46] T. Lamark, T. Johansen, Autophagy: links with the proteasome, Curr. Opin. Cell Biol. 22 (2010) 192–198.

[47] D.A. Butterfield, D. Boyd-Kimball, Amyloid beta-peptide(1–42) contributes to the oxidative stress and neurodegeneration found in Alzheimer disease brain, Brain Pathol. 14 (2004) 426–432.

[48] D.A. Butterfield, T. Reed, S.F. Newman, R. Sultana, Roles of amyloid beta-peptide-associated oxidative stress and brain protein modifications in the pathogenesis of Alzheimer's disease and mild cognitive impairment, Free Radic. Biol. Med. 43 (2007) 658–677.

[49] G. Cenini, G. Maccarinelli, C. Lanni, S.A. Bonini, G. Ferrari-Toninelli, S. Govoni, M. Racchi, D.A. Butterfield, M. Memo, D. Uberti, Wild type but not mutant APP is involved in protective adaptive responses against oxidants, Amino Acids 39 (2010) 271–283.

[50] E.J. Calabrese, L.A. Baldwin, Hormesis as a biological hypothesis, Environ. Health Perspect. 106 (Suppl. 1) (1998) 357–362.

[51] O. Toussaint, J. Remacle, J.F. Dierick, T. Pascal, C. Frippiat, V. Royer, F. Chainiaux, Approach of evolutionary theories of ageing, stress, senescence-like phenotypes, calorie restriction and hormesis from the view point of far-from-equilibrium thermodynamics, Mech. Ageing Dev. 123 (2002) 937–946.

[52] V. Calabrese, C. Cornelius, A.M. Stella, E.J. Calabrese, Cellular stress responses, mitostress and carnitine insufficiencies as critical determinants in aging and neurodegenerative disorders: role of hormesis and vitagenes, Neurochem. Res. 35 (2010) 1880–1915.

[53] V. Calabrese, C. Cornelius, A.T. Dinkova-Kostova, E.J. Calabrese, M.P. Mattson, Cellular stress responses, the hormesis paradigm, and vitagenes: novel targets for therapeutic intervention in neurodegenerative disorders, Antioxid Redox Signal. 13 (2010) 1763–1811.

[54] V. Calabrese, C. Cornelius, A.T. Dinkova-Kostova, I. Iavicoli, R. Di Paola, A. Koverech, S. Cuzzocrea, E. Rizzarelli, E.J. Calabrese, Cellular stress responses, hormetic phytochemicals and vitagenes in aging and longevity, Biochim. Biophys. Acta 1822 (2012) 753–783.

[55] V. Calabrese, C. Cornelius, S. Cuzzocrea, I. Iavicoli, E. Rizzarelli, E.J. Calabrese, Hormesis, cellular stress response and vitagenes as critical determinants in aging and longevity, Mol. Aspects Med. 32 (2011) 279–304.

[56] S. Zhao, E.R. Aviles Jr., D.G. Fujikawa, Nuclear translocation of mitochondrial cytochrome c, lysosomal cathepsins B and D, and three other death-promoting proteins within the first 60 minutes of generalized seizures, J. Neurosci. Res. 88 (2010) 1727–1737.

[57] K. Matsumoto, Y. Akao, H. Yi, M. Shamoto-Nagai, W. Maruyama, M. Naoi, Overexpression of amyloid precursor protein induces susceptibility to oxidative

stress in human neuroblastoma SH-SY5Y cells, J. Neural Transm. 113 (2006) 125–135.

[58] A.J. Yang, D. Chandswangbhuvana, L. Margol, C.G. Glabe, Loss of endosomal/lysosomal membrane impermeability is an early event in amyloid Abeta1-42 pathogenesis, J. Neurosci. Res. 52 (1998) 691–698.

[59] K. Ditaranto, T.L. Tekirian, A.J. Yang, Lysosomal membrane damage in soluble Abeta-mediated cell death in Alzheimer's disease, Neurobiol. Dis. 8 (2001) 19–31.

[60] A.J. Yang, M. Knauer, D.A. Burdick, C. Glabe, Intracellular A beta 1–42 aggregates stimulate the accumulation of stable, insoluble amyloidogenic fragments of the amyloid precursor protein in transfected cells, J. Biol. Chem. 270 (1995) 14786–14792.

[61] B.A. Bahr, K.B. Hoffman, A.J. Yang, U.S. Hess, C.G. Glabe, G. Lynch, Amyloid beta protein is internalized selectively by hippocampal field CA1 and causes neurons to accumulate amyloidogenic carboxyterminal fragments of the amyloid precursor protein, J. Comp. Neurol. 397 (1998) 139–147.